Simulation of hot hole currents in ultra-thin silicon dioxides: The relationship between time to breakdown and hot hole currents

T. Ezaki, H. Nakasato, T. Yamamoto, and M. Hane

Silicon Systems Research Laboratories, System Devices and Fundamental Research, NEC Corporation,
1120 Shimokuzawa, Sagamihara, 229-1198, Japan
E-mail: ezaki@mel.cl.nec.co.jp

***Abstract*- We have investigated the relationship between the currents of hot holes injected into silicon dioxides and the time to break down (T_{BD}) characteristics. The hot hole currents were calculated by combining a tunnel current simulator and a silicon full-band Monte Carlo (FBMC) simulator. Our results show that the hot hole current seems to be responsible for oxide degradation and breakdown. Moreover, the additional impact ionization process where electrons are relaxed into the valence bands plays an important role in hot hole generation in the low-gate-voltage region.**

I. INTRODUCTION

There has been increasing interest in the degradation and breakdown mechanisms of ultra-thin silicon dioxides in the direct tunneling (DT) regime. According to the widely accepted anode hole injection (AHI) model[1], holes generated by the impact ionization of injected electrons can feedback into the oxides. These feedback holes create traps in the oxides, leading to oxide breakdown. In the DT regime, however, the energy of injected electrons is lower than the Si/SiO_2 barrier of 3.1eV (Fig. 1), so the conventional impact ionization process cannot generate holes with energy higher than 2eV (= 3.1eV minus E_g, where E_g is the Si band gap energy of 1.1eV). Thus the hole Si/SiO_2 barrier height of 4.7eV is too high to admit a significant flux of holes. In order to calculate the fed-back hole currents in the low gate bias region, we used the Fermi-level dependent AHI model proposed by Bude *et al.*[2] In this paper we report 1) a simulation of hot hole currents arising from tunneling-electron-initiated impact ionization in ultra-thin dioxides ($t_{ox} = 1.2$ and 1.94nm) by combining quantum mechanical calculations for tunneling currents and the FBMC method for evaluating hole energy distributions in Si substrates and 2) an investigation of the relationship between the hot hole currents and the time-to-breakdown (T_{BD}) characteristics.

II. IMPACT IONIZATION RATE

It has been pointed out [2] that in devices with hole accumulation or inversion layer the additional impact ionization process plays an important role in hot hole generation. Figure 1 schematically shows the ionization processes: (a) is the conventional process [3] and (b) and (c) are the additional processes, where the final states of valence electron lie in the unoccupied valence band states above the Fermi level. As shown in Fig. 1, the maximum energy E_{max} of holes generated by impact ionization is (a) $E_{max} = \varepsilon - E_g$, (b) $E_{max} = \varepsilon + E_g + 2\Delta\varepsilon_F$ and (c) $E_{max} = \varepsilon + \Delta\varepsilon_F$. $\Delta\varepsilon_F$ is the energy distance between the valence band top and the Fermi level. The maximum hole energy due to the additional process in Fig. 1 (b) is $2 \cdot (E_g + \Delta\varepsilon_F) \gtrapprox 2.2\,\text{eV}$ greater than that due to the conventional process. In our FBMC simulation, ionization process shown in Fig. 1 (b) was taken into account as an additional process, because this process may have drastic effect on the anode hot hole generation.

Figure 2 shows the ionization rates as a function of primary electron energy for the conventional and additional processes calculated by using wave functions and a band structure based on the local empirical pseudo-potential model [4, 5]. Ionization rates of the additional process are almost independent of electron energy, which can be explained by using the schematic illustration of the ionization processes shown in Fig. 3. Closed and open circles represent the occupied states and the unoccupied final states of electrons, respectively. In the conventional ionization the number of the final states (open circles in Fig. 3 (a)) decreases with decreasing electron energy, resulting in the diminution of the ionization rates in the low-electron energy region. In the additional ionization, on the other hand, the number of the final states is independent of the primary electron energy. Therefore, the additional ionization rates are constant with respect to the electron energy. As shown in Fig. 2, ionization rates of the additional process are higher than those of the conventional process in the low-electron energy region. This leads us to expect that electrons with energy less than 2eV will tend to select the additional process, resulting in hot hole generation in the low-bias-voltage region. For electrons with energy higher than 3eV, on the other hand, the conventional impact ionization becomes the dominant hole generation process.

III. TUNNELING CURRENT

For accurate simulations of hot hole currents produced by the impact ionization of tunneling electrons injected from the gate region, tunneling electron currents and their

0-7803-6279-9/00/$10.00 © 2000 IEEE

energy spectra at the Si/SiO_2 interface were calculated by solving the Schrödinger and Poisson equations self-consistently. Figure 4 shows experimentally measured and theoretically calculated tunneling currents. Test devices were n^+-poly-gated MOS capacitors with 1.2- and 1.94-nm-thick oxides grown by rapid thermal oxidation at 850℃. Calculated results agree well with experimental data in the $|V_g| > 2$ V region where T_{BD} experiments were performed. Figure 5 shows the band diagram and energy spectrum of the tunneling electron current for the $t_{ox} = 1.2$ nm device at $V_g = -2.8$ V. The DT current flows through the oxide layer in the manner shown in Fig. 5.

IV. Simulation of Hot Hole Currents

FBMC simulations were performed in the Si substrate region in order to obtain the energy distribution of holes. The initial energy distribution of injected electron at the Si/SiO_2 interface is calculated by the following equation

$$n(\varepsilon) = \frac{J_e(\varepsilon)}{e\langle v^+(\varepsilon)\rangle}, \tag{1}$$

where $J_e(\varepsilon)$ is the energy spectrum of tunneling electrons at the interface and $\langle v^+(\varepsilon)\rangle$ is the mean value of the group velocity v in the direction from SiO_2 to Si. The $\langle v^+(\varepsilon)\rangle$ is obtained by

$$\langle v^+(\varepsilon)\rangle = \frac{\sum_{k,i} v(k,i)\,\delta(\varepsilon - \varepsilon(k,i))\,\theta(v(k,i))}{\sum_{k,i} \delta(\varepsilon - \varepsilon(k,i))\,\theta(v(k,i))} \tag{2}$$

$$\theta(v(k,i)) = \begin{cases} 1 & \text{for } v(k,i) \geq 0 \\ 0 & \text{for } v(k,i) < 0 \end{cases}, \tag{3}$$

where k and i are the wave number and band index, respectively.

As shown in Fig. 5 $\Delta\varepsilon_F$ decreases with distance from the interface, so we included in our FBMC simulation the $\Delta\varepsilon_F$ dependency of the additional ionization rates. Quantum yield data for the electron-hole pair-production in Si gives us information about the ratio between the conventional and additional processes. Figure 6 indicates the quantum yield γ, or the average number of electron-hole pairs produced, as a function of gate voltage. Due to the different voltage dependency of γ for the conventional and additional processes, the transition of the dominant hole generation process takes place at $|V_g| \approx 3.4$ V. In the low-voltage region the additional process is the dominant process as shown in Fig. 6. Figure 7 shows the energy distribution of secondary hole after impact ionization. The energy distribution has a large peak at around 3eV, which corresponds to the contribution from the additional ionization process, while the low-energy holes are generated by the conventional process. This means that the additional process has a dramatic impact on hot hole generation in devices with ultra-thin oxides. Hot hole currents were calculated by using the lucky hole model with the image force effect, where the intrinsic barrier height of SiO_2 was assumed to be 4.7eV. Figure 8 shows the hot hole currents as a function of gate voltage. From our simulation, we found that the low-energy hole produced by the conventional process makes no contributions to the hot hole currents. The T_{BD} characteristics are derived from the hot hole currents J_{HH} by using the assumption

$$Q_{HH} = T_{BD} J_{HH} = \text{constant}, \tag{4}$$

where Q_{HH} is the hot hole fluence to break down. Figure 9 shows the T_{BD} as a function of gate voltage, where Q_{HH} is $10^{-4}\,\mathrm{C/cm^{-2}}$. Since the simulation results show good agreement with the measured T_{BD}, the hot hole current injected into silicon dioxides seems to be responsible for oxide degradation and breakdown. As shown in Fig. 9 the slope of the calculated T_{BD} decreases gradually in the $|V_g| > 3.5$ V region, due to the low-energy hole generation by the conventional process.

V. Conclusion

Simulating the hot hole currents in ultra-thin oxides, we found a strong correlation between hot hole currents and oxide lifetimes and found that the additional process plays an important role in hot hole generation in the low-gate-voltage region. We also found a transition in the dominant hole generation process between the conventional and additional processes; this changes the breakdown characteristics between lower- and higher-voltage regions.

References

[1] I. C. Chen, S. Holland, K. K. Young, C. Chang, and C. Hu, Appl. Phys. Lett. 49, 669 (1986).

[2] J. D. Bude, B. E. Weir, P. J. Silverman, IEDM Tech. Dig. 179 (1998).

[3] E. O. Kane, Phys. Rev. **159**, 624 (1967).

[4] M. L. Cohen and T. K. Bergstresser, Phys. Rev. **144**, 789 (1966).

[5] Y. Kamakura, H. Mizuno, M. Yamaji, M. Morifuji, K. Taniguchi, C. Hamaguchi, T. Kunikiyo, and M. Takenaka, J. Appl. Phys. **75**, 3500 (1994).

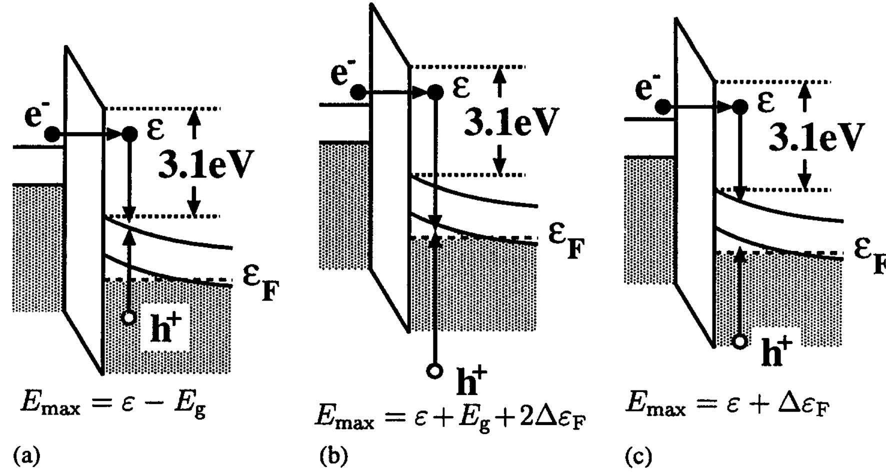

Figure 1: Schematic view of the hole generation processes for the Fermi level dependent AHI model. (a) conventional and (b) and (c) additional impact ionization processes. E_{max} is the maximum energy of holes generated by the impact ionization.

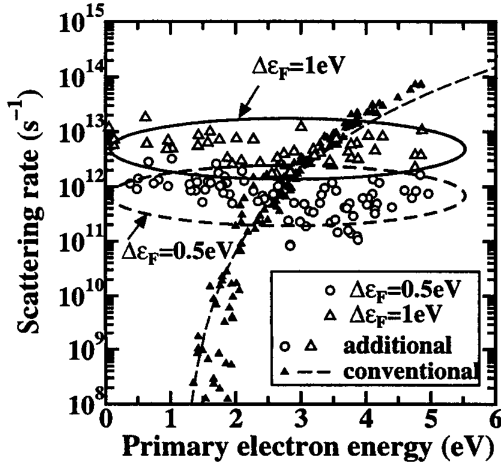

Figure 2: Impact ionization rate calculated by using wave functions and band structure based on local empirical pseudo-potential model.

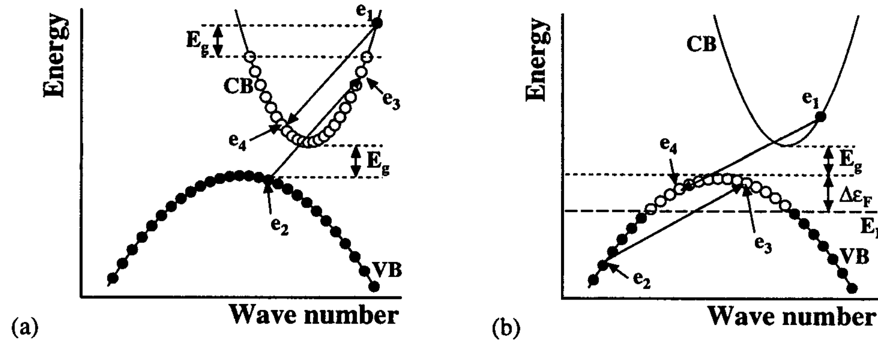

Figure 3: Schematic illustration of (a) the conventional and (b) additional processes. The $(e_1; e_2)$ and $(e_3; e_4)$ are pairs of initial and final electron states, respectively. Closed and open circles represent the occupied states and the final states of electrons, respectively.

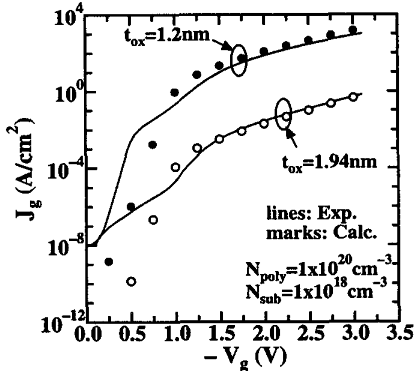

Figure 4: Tunneling currents for SiO_2 films with thickness of t_{ox} = 1.2 and 1.94 nm. Marks indicate experimental data and lines are calculated results.

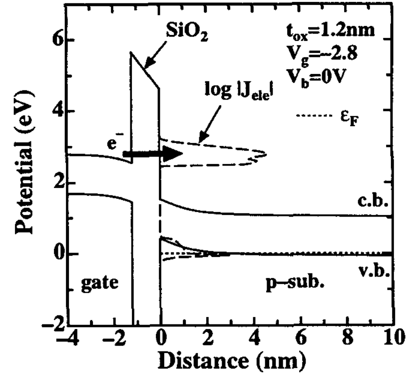

Figure 5: Band diagram (solid line) and energy spectrum of tunneling electron current (dashed line) for t_{ox} = 1.2 nm device at $V_g = -2.8$ V.

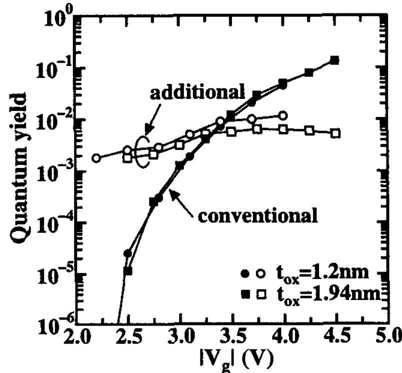

Figure 6: Quantum yields as a function of the gate voltage for the conventional process (solid circles and squares) and additional process (open circles and squares).

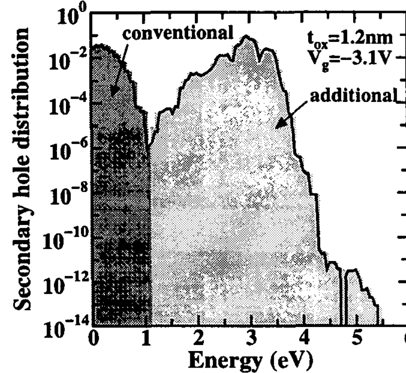

Figure 7: Energy distribution of secondary hole after impact ionization. Dark and light gray areas correspond to contributions from the conventional and additional processes, respectively.

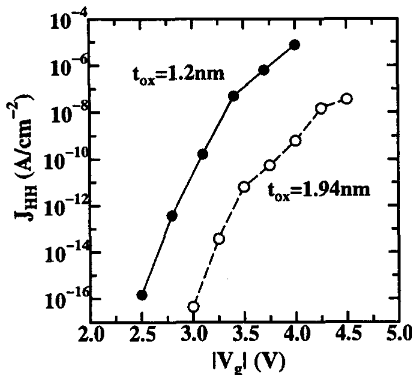

Figure 8: Simulation results of the feedback hot hole currents as a function of gate voltage for t_{ox} = 1.2 nm (solid circles) and t_{ox} = 1.94 nm (open circles).

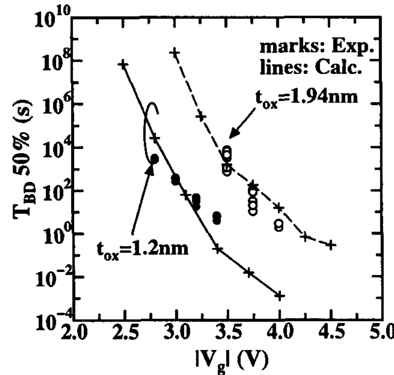

Figure 9: 50% cumulative T_{BD} derived from hot hole currents as a function of gate voltage for t_{ox} = 1.2 nm (solid circles and solid line) and t_{ox} = 1.94 nm (open circles and dashed line).